Observation of Multiple Myosin Subfragment 1–ADP–Fluoroberyllate Complexes by ^{19}F NMR Spectroscopy†

Gillian D. Henry,‡ Shinsaku Maruta,§ Mitsuo Ikebe,‖ and Brian D. Sykes*,‡

Department of Biochemistry and MRC Group in Protein Structure and Function, University of Alberta, Edmonton, Alberta, T6G 2H7, Canada, Department of Bioengineering, Soka University, Hachioji, Tokyo 192, Japan, and Department of Physiology and Biophysics, Case Western Reserve University, Cleveland, Ohio 44106

Received April 30, 1993; Revised Manuscript Received July 12, 1993⊛

ABSTRACT: Fluoroaluminate and fluoroberyllate are potent inhibitors of the ATPase activity of myosin. Inhibition requires the presence of ADP, and much evidence has accumulated to suggest that the tetrahedral fluoroaluminate and fluoroberyllate ions act as phosphate analogues, binding with high affinity at the active site in the position normally occupied by the terminal phosphate of ATP. Both the S1–ADP–fluoroaluminate and the S1–ADP–fluoroberyllate species are thought to resemble kinetic intermediates in the actomyosin ATPase cycle. Characterization of S1-bound fluoroaluminate by ^{19}F NMR is straightforward; a single resonance identified as AlF_4^- is observed easily [Maruta, S., Henry, G. D., Sykes, B. D., & Ikebe, M (1993) *J. Biol. Chem. 268*, 7093–7100]. Bound fluoroberyllate, by contrast, was found to give rise to four separate peaks: a downfield pair at −80 and −83.5 ppm and an upfield pair at −101.5 and −103 ppm, suggesting the existence of four distinct types of S1–ADP–fluoroberyllate complex. The relative intensities of the bound resonances can be altered by changing the F:Be ratio during complex formation. Integration of a spectrum acquired in the presence of a fluorine-labeled nucleotide derivative, 3′(2′)-*O*-(4-fluorobenzoyl)-ADP, in place of ADP yielded a bound fluoride to nucleotide ratio of 1.7–1.9 to 1, showing that the major bound fluoroberyllate species cannot be BeF_3^- as is usually thought. It is proposed that the bound fluoroberyllates correspond to the neutral species $BeF_2(H_2O)_2$ and $BeFOH(H_2O)_2$ and the negatively charged species $[BeF_2OH{\cdot}H_2O]^-$ and $[BeF_3{\cdot}H_2O]^-$, although other possibilities are discussed.

Fluoroaluminate and fluoroberyllate were identified several years ago as potent activators of crude preparations of adenylate cyclase, exerting their effects through a strong association with the α-subunit of the regulatory guanine nucleotide-binding protein (Sternweis & Gilman, 1982). It was subsequently suggested that in the presence of nucleotide diphosphate, the fluorometals behave as phosphate analogues, binding tightly to the active site of the protein in the position normally occupied by the γ-phosphate of GTP (Bigay et al., 1985, 1987; Chabre et al., 1990). Many examples of the association of fluoroaluminate and fluoroberyllate with a wide variety of nucleotide-binding proteins now have been discovered. ATPases such as myosin (Phan & Reisler, 1992; Werber et al., 1992; Maruta et al., 1993), the H^+-translocating (F_1) ATPase (Lunardi et al., 1988), and the Ca^{2+}-ATPase of sarcoplasmic reticulum (Missiaen et al., 1988) are strongly inhibited in the presence of fluoroberyllate or fluoroaluminate and ADP. The slow hydrolysis of nucleotide triphosphate is also inhibited in ATP- and GTP-binding proteins that are not normally classed as enzymes, such as actin and tubulin (Combeau & Carlier, 1989), transducin (Bigay et al., 1987) and many related G-proteins. In all cases, the presence of nucleotide diphosphate is an absolute requirement for the binding of fluoroaluminate or fluoroberyllate.

The ATPase activity of myosin is strongly inhibited by fluoroaluminate and fluoroberyllate. [^3H]ADP is trapped in the active site by both analogues, and measurable dissociation requires several days of dialysis at 4 °C (Maruta et al., 1993). In many respects, the fluorometals resemble orthovanadate (Goodno et al., 1979; Goodno & Taylor, 1982) which is well known as a phosphate analogue and inhibitor of enzyme-catalyzed phosphoryl-transfer reactions. The generally accepted scheme for the hydrolysis of ATP by myosin (M) is

$$M + ATP \underset{k_{-1}}{\overset{k_1}{\rightleftharpoons}} M{\cdot}ATP \underset{k_{-2}}{\overset{k_2}{\rightleftharpoons}} M^*{\cdot}ATP \underset{k_{-3}}{\overset{k_3}{\rightleftharpoons}} M^{**}{\cdot}ADP{\cdot}P_i \underset{k_{-4}}{\overset{k_4}{\rightleftharpoons}}$$
$$M^*{\cdot}ADP{\cdot}P_i \underset{k_{-5}}{\overset{k_5}{\rightleftharpoons}} M^*{\cdot}ADP \underset{k_{-6}}{\overset{k_6}{\rightleftharpoons}} M + ADP$$

where the states M* and M** are distinguished on the basis of enhanced native tryptophan fluorescence. The rate-limiting step is k_4, the conformational change that precedes product release, and the strongly fluorescent M**.ADP.P_i intermediate predominates in solution during steady-state ATP hydrolysis. This conformational change is thought to be equivalent to the power stroke in contracting muscle. Evidence suggests that the S1–ADP–fluoroberyllate and S1–ADP–fluoroaluminate complexes are analogous to intermediate states in the ATPase cycle of myosin, for example, both complexes exhibit enhanced native tryptophan fluorescence comparable with the M**ADP.P_i state (Maruta et al., 1993), and the vanadate cleavage pattern of the S1–ADP–fluorometal complex is similar to that observed for S1 undergoing ATP hydrolysis (Werber et al., 1992). The most important evidence, however, is derived from the study of actin interaction.

† This work was supported by the Medical Research Council of Canada (MRC Group in Protein Structure and Function), the Japan Science Foundation (to S.M.), and NIH Research Grants AR38888 and AR41653 (to M.I.). M.I. is the recipient of an Established Investigator Award from the American Heart Association.

* Address correspondence to this author at the Department of Biochemistry, University of Alberta, Edmonton, Alberta, T6G 2H7, Canada.

‡ University of Alberta.

§ Soka University.

‖ Case Western Reserve University.

⊛ Abstract published in *Advance ACS Abstracts,* September 15, 1993.

0006-2960/93/0432-10451$04.00/0

Nucleotide and actin bind to myosin and its active subfragments in a competitive manner; binding studies have shown that the affinities of both actin and nucleotide for myosin subfragment 1 (S1)[1] are substantially reduced in the ternary complex [Greene & Eisenberg, 1978; reviewed by Goody and Holmes (1983)]. Greene & Eisenberg (1980a) usefully classified the various myosin–nucleotide intermediates in the ATPase cycle as strong- or weak-binding states with respect to actin. M*·ATP or M**·ADP·Pi are weak-binding states whereas M*ADP is a strong-binding state. This can be extended to include nucleotide analogues; for example, the complexes with 5′-adenylyl imidodiphosphate (AMPPNP)[1] and ADP–orthovanadate (Vi) are both weak-binding states (Eisenberg & Greene, 1980b; Goodno & Taylor, 1982).

Addition of excess actin to the S1–ADP–fluoroberyllate complex results in release of the bound nucleotide, a process that can be compared with normal product release, whereas addition of excess fluoroberyllate to acto–S1–ADP results in dissociation of actin from S1 in a manner comparable with the addition of ATP (Maruta et al., 1993). This behavior is easily explained in terms of the competitive binding outlined above; the ternary complex (actin–S1–ADP–fluoroberyllate) is very unstable, and the equilibrium is easily manipulated in favor of one binary complex or the other. The behavior of S1–ADP–fluoroaluminate is more difficult to explain as fluoroaluminate does not dissociate acto–S1–ADP yet in the reverse experiment, a direct binding assay has shown S1–ADP–fluoroaluminate to have a very weak affinity for actin (Maruta et al., 1993). This apparent contradiction is probably explained in terms of the slow kinetics of formation of the S1–ADP–fluoroaluminate complex in the presence of actin, a reaction which may never reach equilibrium under normal experimental conditions. S1–ADP–fluoroaluminate and S1–ADP–fluoroberyllate are thus both properly classified as a weak-binding states. As such, they are potentially useful stable analogues of important kinetic intermediates in the ATPase cycle of myosin.

^{19}F NMR spectroscopy has been used to observe the bound fluorine nuclei in S1–ADP–fluoroaluminate and transducin–GDP–fluoroaluminate (Maruta et al., 1993; Higashijima et al., 1991). In both cases, a single resonance corresponding to bound fluoroaluminate has been identified at a chemical shift well-separated from F^- and the free excess fluoroaluminate species. Using a fluorine-labeled ADP derivative, 3′-(2′)-*O*-(4-fluorobenzoyl)-ADP, it was shown by integration of the ^{19}F NMR spectrum that four aluminium-complexed fluorine atoms exist for each S1-bound nucleotide molecule. The complex is thus correctly written as S1–ADP–AlF_4^-. The ^{19}F nucleus is very sensitive, and spectra of S1-bound fluoroaluminate are very readily obtained in the presence of excess ADP, Al^{3+}, and F^-, even for a protein as large as S1 (110 000 molecular weight). It was somewhat surprising, therefore, that a corresponding S1–ADP–fluoroberyllate signal could not be observed under comparable conditions.

Although protein-bound fluoroberyllate is frequently represented as BeF_3^-, several reports exist to suggest that the situation is actually less straightforward. Denaturation of isolated protein–nucleotide–fluoroberyllate complexes followed by determination of the previously-bound fluoride with an ion-selective electrode has yielded F:Be ratios ranging between 1.7 and 2.8 for actin, tubulin and the mitochondrial F_1 ATPase, the exact value depending on pF and pH (Combeau & Carlier, 1989; Dupuis et al., 1989). In all three cases, the corresponding fluoroaluminate complex yielded F:Al ratios of 4. This has led to the suggestion that BeF_2OH^- (Combeau & Carlier, 1989) or possibly BeF_2 (Dupuis et al., 1989) may be active species in addition to BeF_3^-. In this series of experiments, we have devised conditions for observing S1-bound fluoroberyllate directly using ^{19}F NMR. To our knowledge, these are the first reported NMR spectra of protein-bound fluoroberyllate.

EXPERIMENTAL PROCEDURES

Materials

Skeletal muscle myosin and S1 were prepared by the method of Margossian and Lowey (1982). 2′(3′)-*O*-(4-Fluorobenzoyl)-ATP was synthesized by a modification of the method of Mahmood and Yount (1984) as described by Maruta et al. (1993).

Methods

NMR Spectroscopy. ^{19}F NMR spectra were recorded at 282 MHz on a Varian Unity 300 NMR spectrometer with the acquisition parameters described in the figure legends. The base lines of all spectra were corrected using a backward linear prediction procedure. Chemical shifts are referenced with respect to internal trifluoroacetate at 0 ppm. The sample volume was 2.5 cm^3, and all spectra were recorded at 25 °C.

Sample Preparation. S1 samples were concentrated by dialysis against Aquacide II (Calbiochem) followed by dialysis against 30 mM MOPS buffer, pH 6.8, 180 mM KCl and 1 mM DTT. The S1–ADP–fluoroberyllate complexes were prepared by incubating S1 on ice for 2 h after addition of 1 mM ADP, 5 mM $MgCl_2$, and NaF and $BeSO_4$ at concentrations necessary for the desired Be:F ratio (see figure legends). The excess ADP, fluoride, and fluoroberyllate were then removed by rapid centrifugal gel filtration on Sephadex G50 (Penefsky, 1977), and the S1–ADP–fluoroberyllate complex was transferred immediately to an NMR tube in which the final concentration of buffer and salts was 30 mM MOPS, pH 6.8, 180 mM KCl, 5 mM $MgCl_2$, and 1 mM DTT; 10% D_2O was included for lock purposes. Data collection was started as soon as possible, and always within an hour of the gel filtration step. Samples prepared using 3′(2′)-*O*-(4-fluorobenzoyl)-ADP were prepared similarly, except that a slightly substoichiometric amount of 3′(2′)-*O*-(4-fluorobenzoyl)-ATP was added to S1 and the sample was left to hydrolyze on ice for 10 min before it was added to the solution containing fluoroberyllate as described above.

RESULTS AND DISCUSSION

Behavior of Fluoroberyllate Ions in Solution. Fluoroberyllates form spontaneously in solution when Be^{2+} and F^- ions are mixed; thus, at any given Be:F ratio, a number of species exist in equilibrium (Figure 1). The ^{19}F resonance frequencies of BeF^+ (–97.3 ppm), BeF_2 (–94.5 ppm), BeF_3^- (–92.1 ppm), and BeF_4^{2-} (–90.6 ppm) have been identified previously (Hogben et al., 1972). The multiplet structure of the fluoroberyllate resonances (four peaks of equal intensity) is due to the spin coupling of ^{19}F (spin $^1/_2$) with ^9Be (spin $-^3/_2$). Fluoroberyllates are tetrahedral with the remaining coordination positions occupied by water. The complexes are in slow exchange with each other and with F^- on the chemical shift time scale at 282 MHz, although two-dimensional

[1] Abbreviations: AMPPNP, 5′-adenylyl imidodiphosphate; DTT, dithiothreitol; MOPS, 3-(*N*-morpholino)propanesulfonic acid; NMR, nuclear magnetic resonance; ppm, parts per million; sd, standard deviation; S1, myosin subfragment 1.

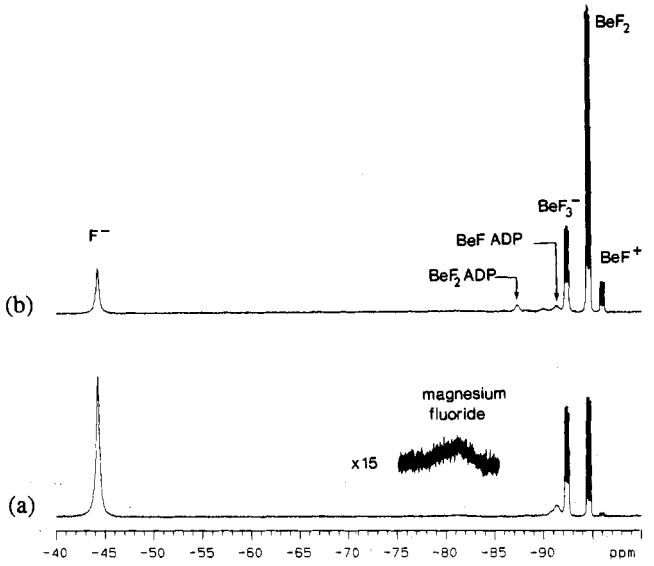

FIGURE 1: ^{19}F NMR spectra of various fluoroberyllate species in equilibrium with free fluoride in the presence of ADP (1 mM) and the absence of protein (25 °C). (a) 5 mM NaF/1 mM $BeSO_4$; (b) 5 mM NaF/5mM $BeSO_4$. Both samples contained 30 mM MOPS, pH 6.8, 180 mM KCl, and 5 mM $MgCl_2$. The broad peaks of low intensity correspond to BeF–ADP (–91.5 ppm) and BeF_2–ADP (–88 ppm) and were assigned according to Issartel et al. (1991). Magnesium fluoride is visible in spectrum a at –80 ppm when the vertical scale is expanded; broadening of the fluoride resonance (–44 ppm) in both spectra is due to chemical exchange with magnesium-bound fluoride. At pH 6.8, contributions to the fluoroberyllate resonances from hydroxyfluoroberyllates are also to be expected (see text). The characteristic multiplet structure of the fluoroberyllates (four resonances of equal intensity) is due to the spin coupling of ^{19}F (spin $^1/_2$) with ^{9}Be (spin $-^3/_2$). Spectra were acquired with a 50° pulse; the acquisition time and the relaxation delay were both set to 0.5 s. A total of 30 000 transients were averaged, and a line broadening of 2 Hz was used.

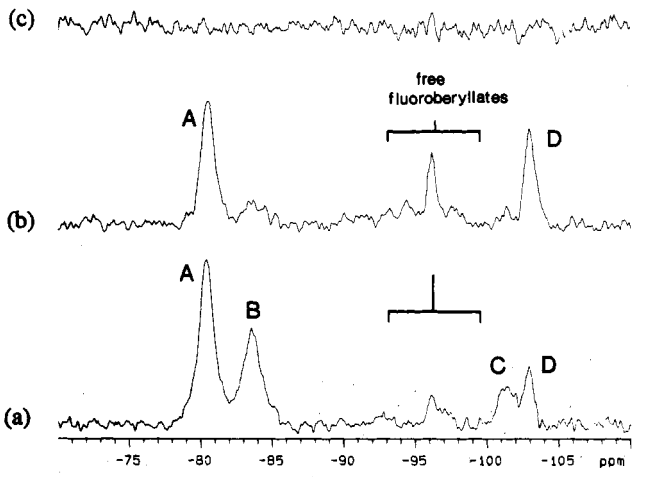

FIGURE 2: ^{19}F NMR spectra (50-Hz line broadening) of S1–ADP–fluoroberyllate formed at pH 6.8. Excess reagents have been removed by gel filtration, although small amounts of free fluoroberyllate are visible in the spectra due to slow dissociation of the complex during the long data acquisition periods. (a) Complex formed in the presence of 5 mM NaF, 1 mM $BeSO_4$, 1 mM ADP, 5 mM $MgCl_2$, 180 mM KCl, 30 mM MOPS, pH 6.8, and 1 mM DTT; (b) as in (a), except the $BeSO_4$ concentration was increased to 5 mM; (c) as in (a), except the ADP was replaced by 1 mM AMPPNP. AMPPNP is not "trapped" by the fluoroberyllate and is removed during the gel filtration step. The protein concentration was 25 mg cm^{-3}, and 81 920 transients were averaged, except for spectrum c where 40 960 transients were averaged. The acquisition time and the delay between transients were both 0.5 s. The S1-bound resonances are much too broad to see F–Be spin coupling, but are typical of the line widths expected for fluorine nuclei associated with a particle the size of S1.

exchange spectroscopy shows that they interconvert rapidly on the T_1 time scale (about 1 s; data not shown). As beryllium (like aluminum) readily forms mixed fluoride–hydroxide complexes, the solution composition also depends on pH (Martin, 1988). pH titrations performed at constant pF suggest that the chemical shift of a given fluoroberyllate species depends on the total charge, for example, BeF_3^-, BeF_2OH^-, and $BeF(OH)_2^-$ cannot be distinguished in the NMR spectrum. A number of weakly associated ADP–fluoroberyllate complexes have been identified (Issartel et al., 1991) which persist at low levels even when Mg^{2+} ions are present (Figure 1).

Although the great majority of complexed fluoride is associated with beryllium, a resonance corresponding to magnesium fluoride (–80 ppm) has also been identified. Magnesium fluoride is in intermediate exchange with free F^- on the chemical shift time scale, as indicated by the substantial broadening of the fluoride resonance (–44 ppm) which always occurs upon addition of Mg^{2+}. As a result of its exchange properties, the appearance of magnesium fluoride can be quite variable, depending strongly on temperature and the Mg^{2+} and F^- ion concentrations (see Figure 1). The addition of ADP reduces the magnesium fluoride contribution; however, the presence of small amounts of magnesium fluoride is a major source of interference in the observation of protein-bound fluoroberyllate resonances.

Observation of S1-Bound Fluoroberyllate. Unlike S1–ADP–fluoroaluminate, which is seen easily in the presence of excess reagents, the S1–ADP–fluoroberyllate complex is not readily observed by NMR under comparable conditions. Furthermore, the large number of resonances present in the absence of protein (Figure 1) makes it difficult to discriminate the bound protein peaks. When the excess reagents are removed, however, a clearer picture emerges. Figure 2a shows the ^{19}F NMR spectrum of S1–ADP–fluoroberyllate prepared by incubation with MgADP and fluoroberyllate at a F^-:Be^{2+} ratio of 5:1 (5 mM NaF/1 mM $BeSO_4$) followed by isolation of the complex by gel filtration (see Methods). It has previously been shown that the S1–ADP–fluoroberyllate complex is very stable, and only free ADP and fluoroberyllate are removed during the gel filtration step. Four distinct bound fluoroberyllate peaks can be seen: a pair of resonances at –80 and –83.5 ppm (labeled A and B, respectively, in Figure 2a), which are downfield of the free fluoroberyllate species, and a second pair of resonances at –101.5 and –103 ppm (labeled C and D), upfield of the free fluoroberyllate. The line widths of these resonances are about 300 Hz, which is consistent with protein-bound fluoroberyllate. None of these resonances were observed when ADP was omitted from the incubation medium (spectrum not shown). Similarly, when ADP was replaced with the nonhydrolyzable analogue 5′-adenylyl imidodiphosphate (AMPPNP), which occupies the γ-phosphate site, no bound fluoroberyllate resonances were seen (Figure 2c). The relative intensities of the bound resonances can be manipulated by altering the F^-:Be^{2+} ratio. Incubation of S1 with a 1:1 F^-:Be^{2+} ratio (5 mM NaF/5 mM $BeSO_4$) increases the relative contributions of resonances A (–80 ppm) and D (–103 ppm), whereas peaks B (–83.5 ppm) and C (–101.5 ppm) are diminished (Figure 2b). On the other hand, increasing the F^-:Be^{2+} ratio from 5:1 to 25:1 makes very little difference to the spectrum (not shown).

To confirm that the four resonances in Figure 2a correspond to genuine S1-bound fluoride, the protein was digested with trypsin, and NMR spectra were recorded as a function of time. All four resonances decreased in intensity as the digestion progressed, and peaks corresponding to F^- and free fluoro-

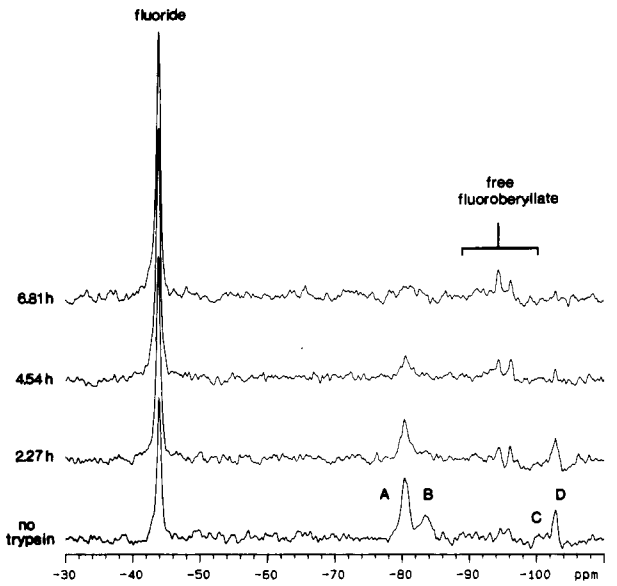

FIGURE 3: Time course of digestion of the S1–ADP–fluoroberyllate complex (formed at a 5:1 F^-:Be ratio as described in the legend to Figure 2) by trypsin (1:50 trypsin:S1 ratio by weight). Both the acquisition time and the delay between transients were 0.5 s; 8192 transients were averaged, and each spectrum required 2.27 h to acquire. F^- and the free fluoroberyllates increase in intensity during the time course of the digestion, whereas bound fluoroberyllates disappear.

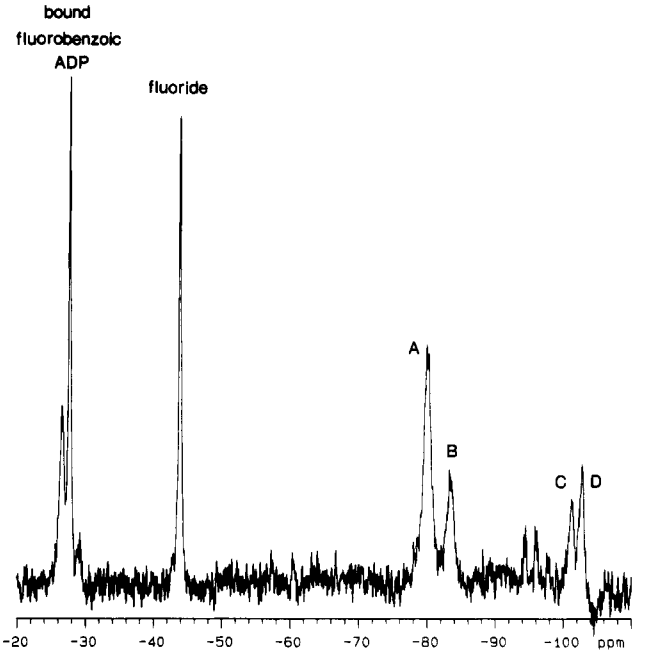

FIGURE 4: ^{19}F NMR spectrum (20-Hz line broadening) of S1–ADP–fluoroberyllate recorded in the presence of 3′(2′)-*O*-(4-fluorobenzoyl)-ADP at pH 6.8. Bound resonances from the fluorinated ADP are at −26.6 and −27.8 ppm. The upfield (−27.8 ppm) resonance is significantly broader than the downfield peak, although the integrals are close to 2:1, suggesting that the two resonances correspond to the 3′ and 2′ isomers of the labeled ADP. When not bound to the protein, these resonate at −29.1 and −29.4 ppm, respectively. The spectrum was recorded with a 90° pulse (23 μs) and an acquisition time of 0.5 s. A relaxation delay of 7 s was included to accommodate the relatively long T_1 of the bound fluorobenzoyl-ADP (0.85 s; the T_1 values of the major bound fluoroberyllate species are between 0.1 and 0.2 s). The transmitter was placed at a point equidistant from the 4-fluorobenzoyl-ADP resonances and those of the major bound fluoroberyllate peaks to ensure equal excitation of the resonances of interest. A total of 10 240 transients (collected as 10 blocks of 1024 to record time-dependent changes) were coadded. The spectrum cannot be integrated directly as the complex slowly dissociates.

beryllate increased accordingly (Figure 3), demonstrating that all four peaks correspond to genuine S1-bound fluoride. There are thus at least four distinct S1–ADP–fluoroberyllate complexes.

It is now apparent why the bound fluoroberyllate signal is comparatively hard to observe; the resonance intensity is distributed between four distinct resonances, and the line widths are significantly broader than the corresponding fluoroaluminate resonance. (Doubling the line width decreases the signal intensity by a factor of 2). Furthermore, the major component of the spectrum (peaks A and B) falls directly on top of the broad magnesium fluoride resonance (Figure 1a) and is typically of comparable intensity. It is also reasonable to consider the possibility that the bound fluoroberyllates contain less fluoride per metal ion than the corresponding fluoroaluminate (AlF_4^-) complex (see below).

Stoichiometry of Fluoride Binding. The first step in identification of the bound species is determination of the total amount of bound fluoride. The fluoride:nucleotide ratio was determined from a spectrum recorded in the presence of a fluorine-labeled ADP analogue, 3′(2′)-*O*-(4-fluorobenzoyl)-ADP. This analogue, which is similar to the fluorescent derivative 3′(2′)-*O*-(*N*-methylanthraniloyl)-ADP (Mant-ADP; Cremo et al., 1990), binds S1 with an affinity comparable to ADP and produces an identical bound fluoroberyllate spectrum. Fluorobenzoyl-ADP was used previously to establish the fluoride:nucleotide ratio (4:1) in the corresponding fluoroaluminate complex. It consists of a 2:1 mixture of the 3′ and 2′ isomers (Maruta et al., 1992), which probably accounts for the presence of two peaks in the spectrum of the S1-bound analogue (Figure 4).

Although isolation of the S1–ADP–fluoroberyllate complex enables observation of the bound fluoroberyllate, the system is no longer at equilibrium and slowly dissociates over the long periods of time (up to 20 h) required to record the NMR spectrum. As the different complexes dissociate at different rates (discussed later), the resonances in Figure 4 cannot be integrated directly; instead, spectra were collected as successive blocks of 1024 transients to record time-dependent changes and resonances in each block integrated separately. The spectrum shown in Figure 4 is the result of the subsequent coaddition of 10 such blocks of data. Assuming dissociation to be a first-order process, the integrals were then extrapolated back to zero time, and these values used to calculate the relative intensities of the four bound fluoroberyllate peaks (Figure 5). Taking into account the small amount of unlabeled ADP (8.6%) in the 3′(2′)-*O*-(4-fluorobenzoyl)-ADP sample, it was calculated that 1.7–1.9 fluorides are bound for each nucleotide. The major source of uncertainty in this experiment arises from the reproducibility of the base-line correction procedures that are necessary for integration of the spectra (see legend to Figure 5). The fluoride:ADP ratio is thus substantially less than 3:1 and means that BeF_3^-, which is usually assumed to be the active species, cannot be the major contributor.

Peak B is particularly susceptible to time-dependent changes (Figure 5), and an average of three measurements gives the rate constant (k_{off}) as 2.3×10^{-5} s^{-1}. The adjacent resonance, peak A, by contrast, does not dissociate measurably during the NMR experiment, suggesting its k_{off} value to be at least 10-fold slower. The upfield resonances are very difficult to quantify because of their weak intensities; however, peak D actually appears to increase in intensity, whereas peak C decreases slowly, resulting in the constant total intensity of Figure 5. This behavior is obviously complex and difficult to interpret. It is possible that the release of a fluoride ion from

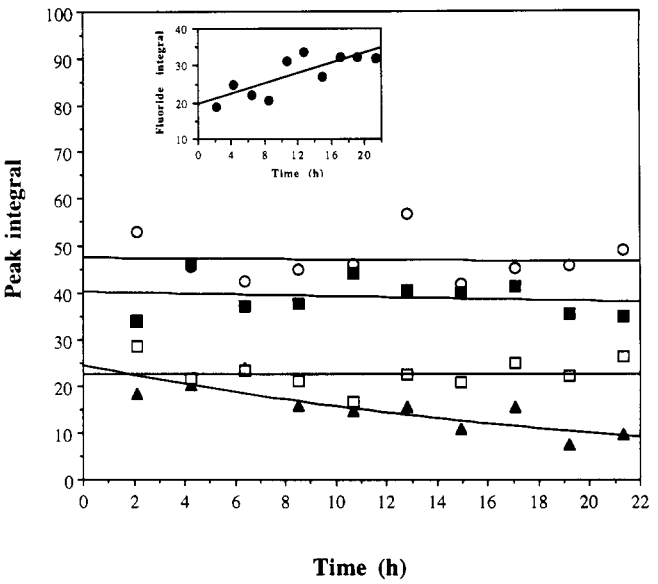

FIGURE 5: Time dependence of the integrals of the bound nucleotide and fluoroberyllate resonances: (○), 3′(2′)-*O*-(4-fluorobenzoyl)-ADP; (■) peak A (–80 ppm); (□) peaks C and D (–101.5 and –103 ppm); (▲) peak B (–83.5 ppm). Each set of data points is fitted to a single exponential decay, but only in the case of peak B is significant dissociation observed. The peak integrals (arbitrary units) extrapolated back to zero time yielded the following values with the standard deviation (sd) of the fit given in parentheses: 47.6 (3.4) for fluorobenzoyl-ADP, 40.3 (2.9) for peak A, 24.5 (2.7) for peak B, and 22.9 (2.4) for peaks C and D. These values were used to calculate the amount of bound fluoride, resulting in a ratio of 1.7 fluorides per bound ADP after the small amount (8.6%) of unlabeled ADP in the sample has been taken into account. The major error in this procedure comes from the base-line correction routines required before the peaks can be integrated. We can estmate, on the basis of repeated integration of the same data, that the true value lies between 1.7 and 1.9 fluorides per bound ADP molecule. The inset shows the corresponding increase in intensity of the F^- peak. The straight line drawn through the data points is intended to guide the eye rather than to imply that the rate is strictly linear.

a more richly fluorinated species (e.g., peak B) results in the increase in intensity of a more poorly fluorinated species (e.g., peak C) although the experiment is insufficiently sensitive for a detailed analysis. Nevertheless, the interpretation of the kinetics of dissociation does not affect the validity of the result.

Origin of the Multiple Bound Fluoroberyllate Resonances. Competition for the active site of S1 between the various fluoroberyllate and hydroxyfluoroberyllate species that are present in equilibrium in free in solution (Figure 1) offers the most straightforward explanation for the presence of the multiple S1–ADP–fluoroberyllate complexes that are observable by ^{19}F NMR. The fact that the relative intensities of the bound peaks can be manipulated by changing the Be:F ratio during complex formation lends considerable support to this interpretation; furthermore, contributions from BeF_2OH^- and BeF_2 in addition to BeF_3^- have already been proposed in other protein systems to explain the variable and nonintegral Be:F ratios measured after chemical denaturation (Combeau & Carlier, 1989; Dupuis et al., 1989). Nevertheless, several other possibilities, which are not necessarily exclusive of the existence of multiple fluoroberyllate species in the γ-phosphate site, will also be considered. These include multiple protein conformational states, covalent bond formation between an ADP β-phosphorus oxygen atom and beryllium, the coordination of partially fluorinated Be^{2+} or Mg^{2+} ions with the oxygen atoms of ADP in the position normally occupied by Mg^{2+} alone, and contributions from inequivalent fluorine atoms in fluoroberyllate ions held rigid at the active site.

Competition between Fluoroberyllate Species. As the dissociation rates of the S1–ADP–fluoroberyllate complexes are very slow, the population distribution between the various species is determined by the relative rates of complex formation. This in turn depends on the concentration of the active species in solution and the rate constant, k_{on}. Although the distribution of the bound fluoroberyllates can be manipulated by altering the F:Be ratio in the initial incubation medium, it is not possible to identify the active species without prior knowledge of the distribution of free fluoroberyllates and hydroxyfluoroberyllates at the appropriate pF and pH. This is not a simple problem as the equilibria are very complex and involve a large number of species.

Hydroxyfluoroberyllates form by the loss of a proton from the hydrated fluoroberyllate complex, i.e., $[BeF_n(H_2O)_{(4-n)}]^{(n-2)-} \rightleftharpoons [BeF_n(H_2O)_{(3-n)}OH]^{(n-1)-} + H^+$; therefore, each reaction has an associated pK_a value. The equilibrium constants and pK_a values for the ternary complexes (i.e., hydroxyfluoroberyllates) in free solution were calculated by Martin (1988) on a statistical basis using the equilibrium constants for the binary complexes, which are known. This is not an unreasonable assumption as F^- and OH^- are isoelectronic; however, these calculations were intended to show the importance of the hydroxy compounds, not to provide a definitive set of equilibrium constants for the interpretation of experimental data. Preliminary experiments using ^{19}F NMR spectroscopy to measure the concentrations of the fluoroberyllate complexes as a function of pH and pF show that the hydroxyfluoroberyllates form more easily than the calculated constants suggest. The statistically-derived equilibrium constants are thus inappropriate for determination of the true concentrations of free species in solution, and as a result it is not possible to identify the bound species simply by appropriate alteration of the solution conditions.

The relatively small amount of bound fluoride (1.7–1.9 fluorine nuclei per ADP molecule) places severe constraints on the possible identities of the bound species. It is immediately apparent that BeF_3^-, which is usually assumed to be the bound anion, is not predominant. Assuming for the moment that all of the bound fluoride exists as fluoroberyllate or hydroxyfluoroberyllate in the γ-phosphate site, then the anions BeF_3^-, BeF_2OH^-, and possibly $BeF(OH)_2^-$ and the neutral species BeF_2 and BeFOH seem to be the most likely contributors. As it seems unlikely that a positively charged molecule would bind tightly at the active site in place of phosphate, BeF^+ can probably be eliminated safely. It might be supposed that the assignments of peaks A–D could be obtained by consideration of the individual peak integrals and the number of bound fluorine atoms required to give the measured amount of total bound fluoride (i.e., 1.7–1.9 fluorine nuclei per ADP). In practice, this was not helpful, and all 24 possible combinations of BeF_3^-, BeF_2OH^-, BeF_2, and BeFOH give an answer within ±20% of the measured value.

Covalent Bond Formation between ADP and Beryllium: Multiple Protein Conformations. It has been suggested repeatedly that fluoroaluminate and fluoroberyllate bind covalently to ADP at the active sites of the fluorometal-binding proteins to form a molecule that resembles ATP [e.g., see Dupuis et al. (1989) and Antonny and Chabre (1991)]. This does not seem to be the case for S1–ADP–AlF_4^-; however, formation of S1–ADP–O–BeF_n could account for the unexpectedly low fluoride to ADP ratio if a fluoride ion was eliminated during complex formation. The possibility of the coexistence of covalently and noncovalently bound complexes and the mechanism of formation of the former raise further

complications for identification of the bound species.

A second major point of interest centers around the large chemical shift difference (about 20 ppm) between the two sets of bound peaks and the fact that the resonance frequencies of peaks A and B are downfield of the free fluoroberyllates whereas those of peaks C and D are upfield. Peaks A and B can be compared with the S1–ADP–AlF_4^- complex, in which the bound fluoroaluminate resonates 12 ppm downfield of the free species (Maruta et al., 1993). Given that the resonances of the free fluoroberyllate species in solution shift predictably downfield upon the addition of each negative charge, this large chemical shift difference is surprising, and may reflect the presence two distinct protein conformations determined by the chemical nature of the bound fluoroberyllate (i.e., number of attached fluorine atoms or the presence or absence of covalent bond formation between Be and ADP). S1–ADP–fluoroberyllate may not, therefore, correspond to a unique conformational state in the ATPase cycle of S1.

Other Possibilities. Several more mundane explanations of the origin of the multiple bound S1–ADP–fluoroberyllate peaks must also be considered. First, the possibility that the fluorine atoms of one or more rigidly bound fluoroberyllate species are inequivalent can be eliminated on the basis of the relative intensities of the different species obtained at different Be:F ratios. The possibility that fluoride is not bound in the γ-phosphate site is more difficult to eliminate. In an extensive NMR study of the interactions of fluoroberyllate with nucleotides and analogues such as pyrophosphate in free solution, Issartel et al. (1991) noted the presence of two complexes in which the fluoroberyllate was partially coordinated by phosphate oxygen atoms of the nucleotide. Although the populations of these complexes are substantially reduced upon addition of Mg^{2+} (Figure 1), it is nevertheless possible that a complex of this type might bind to S1. Perhaps more importantly, one or more fluoride ions may coordinate the Mg^{2+} ion of MgADP in addition to the phosphate oxygen atoms. It is difficult to eliminate either of these possibilities with the available data; however, if the upfield pair of peaks correspond to fluoride that is bound in addition to that found in the γ-phosphate site, then the ratio of bound fluoride to ADP reduces to 1.2, a number that seems unreasonably small.

CONCLUSIONS

S1–ADP–fluoroberyllate can be observed using ^{19}F NMR spectroscopy, although the resonance intensity is much weaker than that of the corresponding S1–ADP–fluoroaluminate complex due to the presence of four bound complexes, a low amount of bound fluoride, and broad line widths. As the relative intensities of the bound resonances can be manipulated by changing the Be:F ratio in the initial incubation medium, it is concluded that the various fluoroberyllate and hydroxyfluoroberyllate complexes present in free solution compete for the active site of S1. The large chemical shift difference between the two sets of bound fluoroberyllate resonances (20 ppm) suggests that more than one protein conformation may be present and that S1–ADP–fluoroberyllate does not represent a unique state in the ATPase cycle of S1.

ACKNOWLEDGMENT

We thank Dr. E. R. Birnbaum of New Mexico State University for calculation of beryllium fluoride species distribution curves and Gerry McQuaid and Don Evjen for continued maintenance of the NMR spectrometer.

REFERENCES

Antonny, B., & Chabre, M. (1992) *J. Biol. Chem. 267*, 6710–6718.
Bagshaw, C., & Trentham, D. R. (1973) *Biochem. J. 133*, 323–328.
Bigay, J., Deterre, P., Pfister, C., & Chabre, M. (1985) *FEBS Lett. 191*, 181–185.
Bigay, J., Deterre, P., Pfister, C., & Chabre, M. (1987) *EMBO J. 6*, 2907–2913.
Chabre, M. (1990) *Trends Biochem. Sci. 15*, 6–10.
Combeau, C., & Carlier, M.-F. (1988) *J. Biol. Chem. 263*, 17429–17436.
Combeau, C., & Carlier, M.-F. (1989) *J. Biol. Chem. 264*, 19017–19021.
Cremo, C. R., Neuron, J. R., & Yount, R. G. (1990) *Biochemistry 29*, 3309–3319.
Dupuis, A., Issartel, J.-P., & Vignais, P. V. (1989) *FEBS Lett. 255*, 47–52.
Goodno, C. C. (1979) *Proc. Natl. Acad. Sci. U.S.A. 76*, 2620–2624.
Goodno, C. C., & Taylor, E. W. (1982) *Proc. Natl. Acad. Sci. U.S.A. 79*, 21–25.
Goody, R. S., & Holmes, K. C. (1983) *Biochim. Biophys. Acta 726*, 13–39.
Greene, L. E., & Eisenberg, E. (1978) *Proc. Natl. Acad. Sci. U.S.A. 75*, 54–58.
Greene, L. E., & Eisenberg, E. (1980a) *Annu. Rev. Physiol. 42*, 293–309.
Greene, L. E., & Eisenberg, E. (1980b) *J. Biol. Chem. 255*, 543–548.
Higashijima, T., Graziano, M. P., Suga, H., Kainosho, M., & Gilman, A. (1991) *J. Biol. Chem. 266*, 3396–3401.
Hogben, M. G., Radley, K., & Reeves, L. W. (1970) *Can. J. Biochem. 48*, 2960–2964.
Issartel, J.-P., Dupuis, A., Morat, C., & Girardet, J.-L. (1991) *Eur. Biophys. J. 20*, 115–126.
Lunardi, J., Dupuis, A, Garin, J., Issartel, J.-P., Michel, L., Chabre, M., & Vignais, P. V. (1988) *Proc. Natl. Acad. Sci. U.S.A. 85*, 8958–8962.
Mahmood, R., & Yount, R. G. (1984) *J. Biol. Chem. 259*, 12956–12959.
Margossian, S. S., & Lowey, S. (1982) *Methods Enzymol. 85*, 55–71.
Martin, R. B. (1988) *Biochem. Biophys. Res. Commun. 155*, 1194–1200.
Maruta, S., Henry, G. D., Sykes, B. D., & Ikebe, M. (1993) *J. Biol. Chem. 268*, 7093–7100.
Missiaen, L., Wuytack, F., DeSmedt, H., Vrolix, M., & Casteels, R. (1988) *Biochem. J. 253*, 827–833.
Penefsky, H. S. (1977) *J. Biol. Chem. 252*, 2891–2899.
Phan, B., & Reisler, E. (1992) *Biochemistry 31*, 4787–4793.
Sternweis, P. C., & Gilman, A. G. (1982) *Proc. Natl. Acad. Sci. U.S.A. 79*, 4888–4891.
Werber, M. M. Peyser, Y. M., & Muhlrad, A. (1992) *Biochemistry 31*, 7190–7197.